

Received: 2020.02.03  
Accepted: 2020.03.19  
Available online: 2020.04.29  
Published: 2020.05.07

# Dietary Melatonin Therapy Alleviates the Lamina Cribrosa Damages in Patients with Mild Cognitive Impairments: A Double-Blinded, Randomized Controlled Study

Authors' Contribution:  
Study Design A  
Data Collection B  
Statistical Analysis C  
Data Interpretation D  
Manuscript Preparation E  
Literature Search F  
Funds Collection G

ABDE 1 **Lei Xu\***  
BCEF 1 **Haixiang Yu\***  
EFG 1 **Hongbin Sun**  
DEFG 2 **Bang Hu**  
CDEG 3 **Yi Geng**

1 Department of Thoracic Surgery, China-Japan Union Hospital of Jilin University, Changchun, Jilin, P.R. China  
2 Department of Colorectal Surgery, The Sixth Affiliated Hospital, Sun Yat-sen University, Guangzhou, Guangdong, P.R. China  
3 Department of Neurosurgery, Liaohe Oil Gem Flower Hospital, Panjin, Liaoning, P.R. China

\* Lei Xu and Haixiang Yu contributed equally to this publication and should be considered as co-first authors

**Corresponding Author:** Hongbin Sun, e-mail: drhongbinsun@163.com, Bang Hu, e-mail: banhuiyao@yeah.net, Yi Geng, e-mail: drgengyi@163.com  
**Source of support:** Departmental sources

**Background:** Alzheimer's disease (AD) is a degenerative disease that is characterized by massive neuron devastations in the hippocampus and cortex. Mild cognitive impairment (MCI) is the transitory stage between normality and AD dementia. This study aimed to investigate the melatonin induced effects on the lamina cribrosa thickness (LCT) of patients with MCI.





**Material/Methods:** The LCT data of patients with MCI were compared to LCT data of healthy controls. Subsequently, all MCI patients were randomly assigned into an experimental group (with melatonin treatment) or a placebo group (without any melatonin treatment).

**Results:** The LCT of MCI patients decreased significantly compared with healthy controls. The univariate analysis showed that the lower the Mini Mental State Examination (MMSE) score ( $P=0.038$ ; 95% CI: 0.876, -0.209), the smaller hippocampus volume ( $P=0.001$ ; 95% CI: -1.594, -2.911), and the upregulated level of cerebrospinal fluid (CSF) T-tau ( $P=0.036$ ; 95% CI: 2.546, -0.271) were associated significantly with the thinner LCT in MCI patients. There were 40 patients in the experimental group and 39 patients in the placebo group. The mean age of the experimental group was not significantly different from the placebo group ( $66.3\pm 8.8$  versus  $66.5\pm 8.3$ ;  $P>0.05$ ). The LCT and hippocampus volume of the melatonin treated group were significantly larger compared with the placebo group ( $P<0.001$ ). On the other hand, the CSF T-tau level of the melatonin treated group was significantly lower compared with the untreated group ( $P<0.001$ ).

**Conclusions:** LCT assessment might allow early diagnosis of MCI. Dietary melatonin therapy could provide an effective medication for MCI patients with LCT alterations.

**MeSH Keywords:** **Diagnostic Techniques, Ophthalmological • Eye Abnormalities • Retinaldehyde**

**Full-text PDF:** <https://www.medscimonit.com/abstract/index/idArt/923232>

 4744  5  1  75



## Background

Alzheimer's disease (AD) is a degenerative disease that is characterized by massive neuron devastations in the hippocampus and cortex. As a typical dementia in the central nervous system (CNS), the AD has an incidence rate of approximately 10% in the elderly population worldwide [1]. Mild cognitive impairment (MCI) is the transitory stage between normality and AD dementia. It is a heterogeneous condition that may precede diseases other than AD and with different pathologies [2]. As a prodromal stage of AD, MCI patients have a high risk of progressing into AD. In the past decades, MCI has earned abundant interest from epidemiological and pathological studies [3]. This disease can devastate cognitive function, alter personality, and impair daily quality of life. However, the pathological damage of MCI and early AD are difficult to differentiate. Accumulating evidence suggests that AD patients may always have had evident visual function impairments, implicating that they might have undergone some disruptions in the visual system [4]. A pioneering histological study found retinal ganglion cell (RGC) degeneration and optic nerve trophic in MCI patients, indicating a definite relationship between visual system degeneration and AD pathology [5]. Generally, AD is diagnosed based on a combination of clinical symptoms, biomarkers, and imaging examinations. However, these examinations are expensive and invasive, and might cause potential discomfort or suffering in patients. AD patients are always diagnosed at late stages when they already have terrible symptoms. On the other hand, pathological changes, such as amyloid beta (A $\beta$ ) plaques and neurofibrillary tangles (NFT), begin as early as 20 years before symptom onset [6]. Consequently, it is imperative to develop a noninvasive, rational, and reliable approach that would be helpful for the efficient diagnosis of MCI.

Retina is type of neural tissue that is considered a peripheral element of the CNS [7,8]. The optic nerve derives from the RGC axons that is located in the innermost layer of retina. This cranial nerve tissue shares many similarities with brain tissue [9]. Accordingly, retina and optic nerve might be involved in the pathological processes of CNS disorders. For instance, retinal degeneration occurs in patients with neurodegenerative disorders, and shares mutual pathogenic mechanisms to some extent [10]. Therefore, the pathological characteristics of CNS disease might manifest in the retina. It is rational to assess the retina which is considered a continuum of the CNS and has several similarities with the brain. The lamina cribrosa (LC) is the site where optic nerve axons of the retina run through it, and it is vulnerable to axonal damage [11]. Several ophthalmological studies have shown that the LC is severely damaged during RGC axonal loss [12,13]. Patients with Parkinson's disease or glaucomatous nerve fiber damage are reported to have thinner LC. Consequently, examination of the LC may afford instrumental information on the pathological procession

of CNS disease. In the past decades, spectral-domain optical coherence tomography (SD-OCT) has been used as a diagnostic approach for retinopathy and optic neuropathies [14]. Particularly, SD-OCT can produce cross-sectional images of the LC *in vivo*. With the assistance of this approach, retinopathies such as posterior laminar displacement and focal LC damage in human eyes can be discovered efficiently [15,16]. Thus, in this study, we aimed to analyze the LC in MCI patients via SD-OCT examination.

Biomarkers can be used to objectively evaluate the pathological processes of CNS disorders [17]. Generally, biomarkers include neuroimaging, biochemical, and genetic biomarkers. Some neuroimaging modalities, such as the electroencephalography (EEG) and magnetoencephalography (MEG), are economical, non-invasive tools used to study the dynamic changes of the brain [18,19]. Event-related potential (ERP) is electrical activity produced by the brain time-locked to sensory, cognitive, or motor stimulus. EEG and ERP reliably reflect the synaptic transmission processes, and they seem to be particularly suitable for studying the disorder of synaptic plasticity of AD [20]. Several promising indices of EEG and ERP have been put forward as functional biomarkers of synaptic neurotransmission in AD. The spectral power and coherence in different frequency bands can offer effective tools for diagnosing AD. Correlation dimension, multi-scale entropy, and complexity measurements are frequently used EEG parameters [21,22]. For instance, EEG studies have shown that reduced alpha power and increased delta are the most prominent features of AD patients [23]. Moreover, the severity of P300 abnormality is associated with impaired memory and cognition in AD patients [24]. These functional biomarkers could open a new window to objectively assess the neuronal activities associated with AD and MCI.

Although the EEG/MEG-based neuromarkers are effective indicators to assess the disease progression status, they do not directly reflect the pathological characteristics of lesions in the brain. As reported by a series of research studies, a huge variability is implicated in the predictive algorithms of both EEG and MEG [20,25]. Therefore, it is urgently needed to search for neuromarkers that are the most rational for application in clinical practice. A possible biomarker for staging the neuropathological lesions in AD is melatonin. Melatonin is a pineal hormone that is involved in circadian rhythms, and may also exert neuroprotective effects on AD [26]. A recent clinical study showed that the cerebrospinal fluid (CSF) levels of melatonin are decreased significantly in the temporal cortex of aged AD patients, highlighting that changes in CSF melatonin levels may be a pioneering event even before clinical symptoms occur in AD patients [27]. Another study showed that the melatonin receptors in AD patients were impaired with severe consequences of pathologies and clinical symptoms [28]. The variations

related to melatonin receptor type 1A gene (MTNR1A) should be considered as a shared genetic risk factor for AD in aged populations [29]. Therefore, melatonin might act as a diagnostic marker for disorders in the neuro-immuno-endocrine system. Pioneering research has shown that exogenous melatonin supplements could confer cytoprotection on ocular cells [30–32]. Our study aimed to explore whether melatonin induced beneficial effects on the LC of MCI patients. We aimed to show that LC assessment using the noninvasive imaging technique can act as an auxiliary diagnosis method of MCI, and facilitate preventive measures against disease progression. The dietary melatonin therapy could therefore increase LCT and reduce CSF T-tau levels of MCI patients. Thus, this study data could enrich our understandings about melatonin and could shed light on developing an effective therapy for MCI patients with LC alterations.

## Material and Methods

### Study design

The study protocol followed the Declaration of Helsinki and was approved by the ethics review committee of Liaohe Oil Gem Flower Hospital and Jinzhou Medical College (No. 201815069). MCI patients were consecutively recruited from the Liaohe Oil Gem Flower Hospital and enrolled between September 2017 and December 2018. Age matched volunteers were enrolled and establish a control group. All participants received oral and written information about the study, and each participant provided written informed consent. Their common data including age, sex, education background, systemic hypertension, intraocular pressure (IOP), axial length, and central corneal thickness (CCT) were thoroughly recorded. The educational level of these participants was classified as the primary school (0 to 6 years), secondary school (6 to 15 years), and high school (>15 years) following a previously described method [33].

### Inclusion and exclusion criteria

The diagnosis of MCI was based on the 4th edition Diagnostic and Statistical Manual of Mental Disorders (DSMIV). The cognition function of participant was evaluated by the Mini Mental State Examination (MMSE) [34]. These patients scoring 24 to 30 points were classified as having MCI. Magnetic resonance imaging (MRI) examination was performed to exclude other diseases of the CNS. Inclusion criteria included the following: patient complaints in memory items corroborated by a relative; the patient was not normal nor demented; abnormal performance in the delayed recall; normal general cognitive function; instrumental activities of daily living were generally good. Exclusion criteria were as follows: patients younger than 65 years or older than 75 years, with alcohol addiction,

memantine drug usage, metabolic syndrome, Parkinson's disease, mental disease, hallucinations, history of ischemic or hemorrhagic stroke. All participants underwent ophthalmic examinations, and patients have corneal pathology, dense media opacities, history of uveitis, glaucomatous optic neuropathy, or congenital abnormal optic disc were excluded from this study. Patients with concomitant ocular disease and systemic medication known to affect the IOP were also excluded from this study. Using the same exclusion criteria, the control participants were recruited from healthy volunteers who had no cognitive complaint, systemic, neurologic, or ophthalmic disease history.

### Pharmacological administration

All the recruited MCI patients were randomly assigned to receive melatonin (experimental group) or placebo capsules (placebo group). Experimental participants received melatonin (at the dose of 0.15 mg/kg) for consecutively 6 months, while the placebo group received lactose placebo capsules. The melatonin or placebo was given at 20:30 pm. All participants received 2 hours of usual indoor light exposure (150–200 lux) before taking the drugs. The drugs were administrated in a double-blind design by randomized allocation. All participants were to undergo a follow-up colonoscopy 1 year after enrolment.

### MRI examination

MRIs are segmented at different scales using non-local patch based multi-atlas methods. All structure segmentations are based on volBrain expert definition. Neuroimaging was performed using a 1.5 T Siemens Aera scanner (Siemens, Germany). Structural images were acquired using T1-weighted 3D Magnetization Prepared Rapid Gradient Echo (MPRAGE) sequence in sagittal plane. The MR T1 data was downloaded from PACS server, transferred and processed using different software. MR data was converted to NIFTI format for volume analysis. The volBrain analysis system was used to calculate hippocampal volume. This system works remotely through a web interface using a SaaS (Software as a Service) model following a previously described method [35].

### SD-OCT examination and measurements

NSD-OCT (Tomey, Ultrasonic Pachymetry, Germany) with an enhanced depth-imaging program was used to quantify the LCT of each participant. The protocol for SD-OCT scanning and LCT analysis followed a previously described method [5]. Briefly, 1% tropicamide solution was used to dilate the pupils before examination. Scanning laser images were properly aligned with the optical nerve head (ONH) in the center of the scan. From these horizontal B scans, we selected 3 frames (center, mid-superior, and mid-inferior) that passed through the ONH. Figure 1A illustrates the

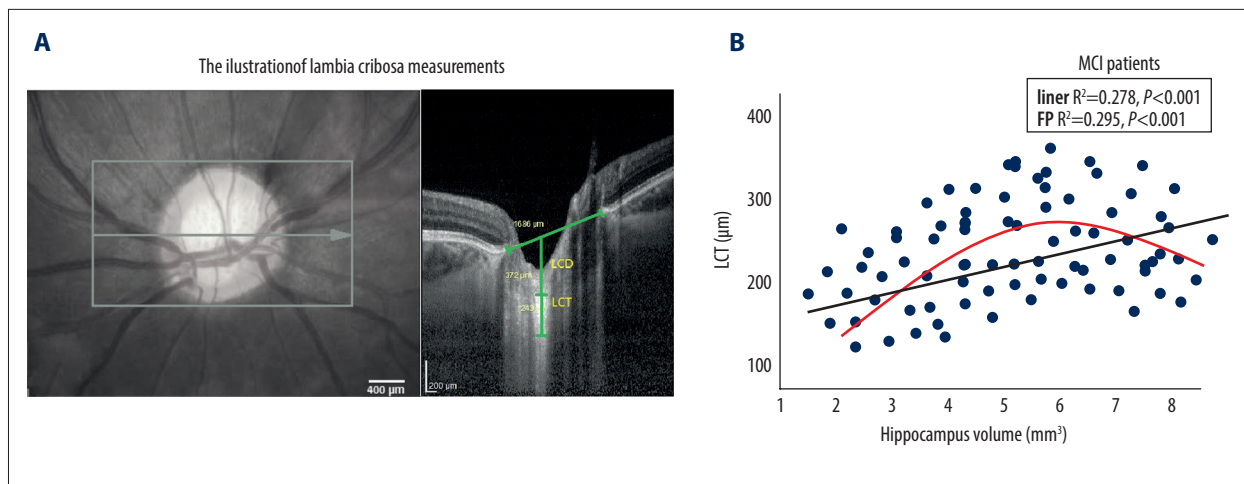


**Figure 1.** (A) VolBrain analysis system was used to analyze the hippocampal volume. MRIs were segmented at different scales using non-local patch-based multi-atlas methods. The intracranial cavity was extracted, and 8 subcortical structures were segmented including: lateral ventricles, caudate nucleus, putamen, thalamus, globus pallidus, hippocampus, amygdala, and nucleus accumbens. (B) LC measurements via the enhanced depth imaging SD-OCT. Anterior and posterior borders of the highly reflective region at the vertical center of the ONH in the horizontal cross-section images were defined as LCT boundaries, and the distance between them was defined as LCT. MRI – magnetic resonance imaging; LC – lamina cribrosa; LCT – lamina cribrosa thickness; SD-OCT – spectral-domain optical coherence tomography; ONH – optical nerve head.

LCT borders and Bruch membrane opening (BMO) in ONH OCT images of an AD patient and a normal control. Measurements were acquired using HEYEX software 6.0 (Heidelberg Engineering Inc., Heidelberg, Germany). High resolution images of the choroid and retinal nerve fiber layer (RNFL) were obtained with using affiliated imaging protocols of OCT. Choroid thickness was measured with horizontal B-scans on vertical lines running towards the choriocleral junction. The outer boundaries of the visible choroid vessels were considered the choriocleral junction. In the measurement of circumpapillary RNFL, radial scans were visualized with the shadow-removal functionality protocol. Each measurement was performed 3 times by the same examiner, and the mean value was calculated

### CSF protein analysis

CSF specimens were harvest via fluoroscopy-guided lumbar puncture technique. The CSF analysis was performed by board-certified laboratory technicians who were blinded to the group information and clinical diagnoses. The expression levels of tau (T-tau), amyloid-beta 1-42 peptide (A $\beta$ 1-42), and tau phosphorylated at threonine 181 (P-tau181P) in the CSF samples were analyzed using the commercially available Luminex® 200™ assays (Luminex, Austin, TX, USA). A quality control sample was evaluated in duplicate on each run used to complete the analysis.

### Statistical analysis

The analysis of LCT and LCD was conducted by the same examiner using similar class measurement parameters in these selected

eyes. The numeric data are presented as mean $\pm$ standard deviation (SD). Qualitative variables are presented as count and percent. Chi-square test was used to compare the enumeration data between groups. For categorical variables, Pearson's chi-square test and Fisher's exact test were performed for parametric and nonparametric comparisons, respectively.  $P<0.05$  was considered to have statistically significance.

## Results

In total, 85 patients diagnosed as MCI were initially involved in this study. Of these 85 patients, 4 patients (4.70%) were excluded for the concurrent ophthalmic complications (glaucoma); 2 patients (2.35%) were excluded for the poor imaging quality of the LC borders beneath the vascular structures, yielding a final sample of 79 MCI patients for final analysis. Seventy-nine healthy age-matched volunteers who met the same inclusion criteria were recruited for this study, and none was excluded. Bilateral eyes of each participant were examined and subjected to further analysis.

The basic characteristics and ophthalmological data of the MCI patients and healthy controls are summarized in Table 1. The MMSE score of the healthy control group (28.86 $\pm$ 1.53) was significantly larger compared with the MCI group (22.09 $\pm$ 3.05;  $P<0.001$ ). The mean age was 66.7 $\pm$ 8.6 years in the MCI group (38 males and 41 females), and 66.0 $\pm$ 8.3 years in the healthy control group (39 males and 40 females), with no statistical difference between the 2 groups ( $P=0.68$ ). The Best-Corrected

**Table 1.** Demographic characteristics in MCI patients and healthy controls.

	Healthy (n=79)	MCI (n=79)	P value
Age	66.0±8.3	66.7±8.6	0.684
Gender (Male/Female)	39: 40	38: 41	0.930
Education levels	19: 36: 24	18: 35: 26	0.276
MMSE score	28.86±1.53	22.09±3.05	<0.001
BCVA	0.08±0.05	0.07±0.06	0.841
Refractive error	0.17±1.63	0.26±1.81	0.582
VDD (μm)	1741.9±155.8	1750.2±167.3	0.964
HDD (μm)	1573.3±139.8	1562.9±165.2	0.891
Axial length (mm)	23.29±0.63	23.56±0.76	0.650
IOP (mmHg)	14.96±3.18	14.55±3.21	0.592
CCT (μm)	539.17±30.09	537.60±28.52	0.922
RNFL thickness (μm)	103.7±13.0	86.2±9.9	<0.001
Choroid thickness			
Sub-foveal (μm)	249.5±30.1	232.4±29.7	<0.001
Temporal (μm)	228.0±25.6	221.5±21.0	0.684
Nasal (μm)	216.7±21.8	213.3±20.5	0.761

Data are presented as the mean±standard deviation unless otherwise specified. MCI – mild cognitive impairment; IOP – intraocular pressure; BCVA – Best-Corrected Visual Acuity; VDD – vertical disc diameter; HDD – horizontal disc diameter; MMSE – Mini-Mental Status Examination; RNFL – retinal nerve fiber layer; CCT – central corneal thickness.

Visual Acuity (BCVA) score was at least 6 out of 10 in all participates, with no statistical difference between the 2 groups ( $P=0.84$ ). The refractive error (measured as mean spherical lens equivalent), was  $0.17\pm 1.63$  D in the healthy controls, and  $0.26\pm 1.81$  D in the MCI group ( $P=0.58$ ). The axial length (mm) was  $23.29\pm 0.63$  mm in the healthy controls and  $23.56\pm 0.76$  mm in the MCI group ( $P=0.65$ ). Educational level of the 2 groups did not significantly differ from each other ( $P=0.27$ ). The IOP (mmHg) was  $14.96\pm 3.18$  mmHg in the healthy controls and  $14.55\pm 3.21$  mmHg in the MCI group ( $P=0.59$ ). The central corneal thickness was  $539.17\pm 30.09$  μm in the healthy control group and  $537.60\pm 28.52$  μm in the MCI group ( $P=0.92$ ). The vertical disc diameter (VDD) was  $1741.9\pm 155.8$  μm in the healthy group and  $1750.2\pm 167.3$  μm in the MCI group ( $P=0.96$ ). The horizontal disc diameter (HDD) was  $1573.3\pm 139.8$  μm in the healthy control group and  $1562.9\pm 165.2$  μm in the MCI group ( $P=0.89$ ). The retinal nerve fiber layer (RNFL) thickness was  $103.7\pm 13.0$  μm in the healthy group and  $86.2\pm 9.9$  μm in the MCI group ( $P<0.001$ ). The choroid thicknesses at subfoveal region was  $249.5\pm 30.1$  μm in the healthy control group and  $221.3\pm 26.9$  μm in the MCI group ( $P<0.001$ ). The choroid thicknesses at temporal region was  $228.0\pm 25.6$  μm in the healthy control group and  $221.5\pm 21.0$  μm in the MCI group ( $P=0.684$ ). The choroid thicknesses at nasal region was  $216.7\pm 21.8$  μm in the healthy control group, and  $213.3\pm 20.5$  μm in the MCI group ( $P=0.761$ ).

The hippocampal volume of participates are presented in Table 2. The total hippocampal volume of the healthy control group was significantly higher compared with the MCI group ( $7.73\pm 0.61$  mm<sup>3</sup> versus  $6.41\pm 0.52$  mm<sup>3</sup>;  $P<0.001$ ). In greater detail, the hippocampal volumes of each lobe were separately analyzed. The right and left hippocampal volumes were  $3.85\pm 0.36$  and  $3.82\pm 0.33$  in the MCI group, while  $3.29\pm 0.21$  and  $3.26\pm 0.22$  in the healthy control group ( $P<0.001$ ). The CSF pressure was  $13.1\pm 2.2$  mmHg in the healthy group and  $13.6\pm 2.5$  mmHg in the MCI group ( $P=0.24$ ). In the CSF proteins analysis, the Aβ<sub>1-42</sub> level was  $471.25\pm 130.79$  pg/mL in the healthy group and  $338.51\pm 122.05$  pg/mL in the MCI group ( $P<0.001$ ). The T-tau level was  $64.09\pm 18.21$  pg/mL in the healthy group and  $93.18\pm 25.01$  pg/mL in the MCI group ( $P<0.001$ ). The P-tau<sub>181P</sub> level was  $25.49\pm 12.06$  pg/mL in the healthy group and  $36.64\pm 15.23$  pg/mL in the MCI group ( $P<0.001$ ).

The mean LCT was  $228.03\pm 16.65$  μm in the MCI group and  $246.25\pm 16.08$  μm in the healthy control group ( $P<0.001$ ). In greater detail, the thickness of superior, central, inferior LC was separately analyzed and compared. The superior LCTs were  $230.81\pm 15.92$  μm in the MCI group, and  $209.25\pm 15.80$  μm in the healthy control group ( $P<0.001$ ). The central LCTs were  $246.61\pm 17.06$  μm in the MCI group, and  $259.82\pm 16.91$  μm in the healthy control group ( $P<0.001$ ). The inferior LCT were

**Table 2.** Hippocampal volumes and LCT measurements in MCI patients and healthy controls.

	Healthy (n=79)	MCI (n=79)	P value
<b>Hippocampus</b>			
Total (mm <sup>3</sup> )	7.73±0.61	6.41±0.52	<0.001
Right (mm <sup>3</sup> )	3.85±0.36	3.29±0.21	<0.001
Left (mm <sup>3</sup> )	3.82±0.33	3.26±0.22	<0.001
<b>CSF</b>			
Pressure (mmHg)	13.1± 2.2	13.6±2.5	P=0.24
Aβ1-42 (pg/mL)	471.25±130.79	338.51± 122.05	<0.001
T-tau (pg/mL)	64.09±18.21	93.18±25.01	<0.001
P-tau181P (pg/mL)	25.49±12.06	36.64±15.23	<0.001
<b>LCT (μm)</b>			
Superior	230.81±15.92	209.25±15.80	<0.001
Central	259.82±16.91	246.61±17.06	<0.001
Inferior	238.06±18.25	221.62±17.21	<0.001
Average	246.25±16.08	228.03±16.65	<0.001
LCD (μm)	436.54±77.29	433.69±87.70	0.72

Data are presented as the mean±standard deviation unless otherwise specified. MCI – mild cognitive impairment; Aβ1-42 – amyloid β1-42; CSF – cerebrospinal fluid; LCD – lamina cribrosa depth; LCT – lamina cribrosa thickness.

221.62±17.21 μm in the MCI group and 238.06±18.25 μm in the healthy control group (*P*<0.001). These findings suggested that the LCT at 3 locations (superior, central, and inferior) were significantly larger in the healthy control group than those in the MCI group. The LCD was 433.69±87.70 μm in the MCI patients, and 436.54±77.29 μm in the healthy controls (*P*=0.72). Furthermore, our data suggested that LCT decreased in parallel with the reduced hippocampal volume, indicating a significant correlation (*P*<0.001, Table 3). In the patients with MCI, the univariate analysis revealed that a lower MMSE score (*P*=0.038; 95% CI: 0.876, -0.209), a smaller hippocampus volume (*P*=0.001; 95% CI: -1.594, -2.911), higher level of CSF T-tau (*P*=0.036; 95% CI: 2.546, 0.271) were associated significantly with the thinner LCT. In multivariate analysis, the LCT was influenced significantly by the CSF T-tau level (*P*=0.041; 95% CI: 2.109, 0.562) and hippocampus volume (*P*<0.001; 95% CI: -1.082, 2.114). The relationship between LCT and hippocampus volume was significant for both a linear model (*R*<sup>2</sup>=0.278, *P*<0.001; Figure 1B, black line) and a nonlinear model (*R*<sup>2</sup>=0.295, *P*<0.001; red line).

In the therapeutic trial, the MMSE score of the melatonin treated group (23.19±2.06) was significantly larger compared with the placebo group (20.56±2.17; *P*<0.001, Table 4). The mean age, educational level, IOP, BCVA, refractive error, the axial length, central corneal thickness, VDD, HDD, and choroid thicknesses

were not significantly different between the 2 groups. The RNFL thickness was 82.6±9.1 μm in the melatonin treated group, and 76.8±8.3 μm in the placebo group (*P*<0.001). The total hippocampal volume of the melatonin treated group was significantly higher compared with the placebo group (6.71±0.39 mm<sup>3</sup> versus 6.49±0.32 mm<sup>3</sup>; *P*<0.001; Table 5). The right and left hippocampal volumes were 3.85±0.36 and 3.82±0.33 respectively in the melatonin treated group, while 3.38±0.31 and 3.36±0.29 respectively in the placebo group (*P*<0.001). In the CSF proteins analysis, the Aβ1-42 level was 329.62±117.59 pg/mL in the melatonin treated group and 310.82±118.66 pg/mL in the placebo group (*P*<0.001). The T-tau level was 95.05±22.94/mL in the melatonin treated group and 108.29±17.60 pg/mL in 329.62 (*P*<0.001). The P-tau181P level was 38.27±13.80 pg/mL in the melatonin treated group and 45.08±12.73 pg/mL in the placebo group (*P*<0.001). The LCD was 435.80±70.18 μm in the melatonin treated group, and 432.65±68.24 μm in the placebo group (*P*=0.72). The mean LCT was 226.89±16.02 μm in the melatonin treated group and 215.42±15.28 μm in the placebo group (*P*<0.001). The superior LCTs were 206.91±14.55 μm in the melatonin treated group, and 195.29±15.10 μm in the placebo group (*P*<0.001). The central LCTs were 246.83±16.02 μm in the melatonin treated group, and 238.50±13.79 μm in the placebo group (*P*<0.001). The inferior LCT were 220.54±15.16 μm in the melatonin treated group and 205.08±14.21 μm in the placebo group (*P*<0.001). These findings suggested that the LCT at different

**Table 3.** Factors associated with the lamina cribrosa thickness in MCI patients.

	Univariate analysis			Multivariate analysis		
	$\beta$	(95% CI)	P value	$\beta$	(95% CI)	P value
MMSE score	0.552	0.876, 0.209	0.039	0.401	0.738, 0.217	0.096
RNFL thickness ( $\mu\text{m}$ )	2.318	3.628, 1.294	0.615	–	–	–
Choroid thickness	0.861	–1.251, 2.687	0.321	–	–	–
Hippocampus volume	0.631	–1.309, 2.209	0.001	0.545	–0.971, 1.883	0.001
A $\beta$ 1–42 (pg/mL)	–0.139	–2.597, 2.150	0.356	–	–	–
T-tau (pg/mL)	–0.629	–0.985, 1.372	0.005	–0.496	–0.746, 1.104	0.059
P-tau181P (pg/mL)	3.769	6.530, 1.561	0.028	2.984	5.671, 1.309	0.085

Data are presented as the mean $\pm$ standard deviation unless otherwise specified. MCI – mild cognitive impairment; BMI – body mass index; IOP – intraocular pressure; MMSE – Mini-Mental Status Examination; RNFL – retinal nerve fiber layer; A $\beta$ 1–42 – amyloid  $\beta$ 1–42.

**Table 4.** Demographic characteristics of melatonin group and placebo group.

	Melatonin (n=40)	Placebo (n=39)	P value
Age	66.3 $\pm$ 8.8	66.5 $\pm$ 8.3	0.838
Gender (Male/Female)	21: 19	21: 18	0.951
Education levels	7: 16: 13	10: 15: 11	0.276
MMSE score	23.19 $\pm$ 2.06	20.56 $\pm$ 2.17	<0.001
BCVA	0.09 $\pm$ 0.03	0.08 $\pm$ 0.05	0.795
Refractive error	0.24 $\pm$ 1.51	0.26 $\pm$ 1.69	0.806
VDD ( $\mu\text{m}$ )	1748.2 $\pm$ 150.6	1746.0 $\pm$ 155.8	0.923
HDD ( $\mu\text{m}$ )	1569.8 $\pm$ 149.1	1555.3 $\pm$ 152.5	0.864
Axial length (mm)	23.38 $\pm$ 0.66	23.51 $\pm$ 0.69	0.713
IOP (mmHg)	14.83 $\pm$ 3.06	14.60 $\pm$ 3.18	0.607
CCT ( $\mu\text{m}$ )	535.94 $\pm$ 31.52	538.80 $\pm$ 26.91	0.896
RNFL thickness ( $\mu\text{m}$ )	82.6 $\pm$ 9.1	76.8 $\pm$ 8.3	<0.001
Choroid thickness			
Sub-foveal ( $\mu\text{m}$ )	231.6 $\pm$ 28.13	223.9 $\pm$ 24.6	<0.001
Temporal ( $\mu\text{m}$ )	208.3 $\pm$ 20.1	195.3 $\pm$ 16.9	<0.001
Nasal ( $\mu\text{m}$ )	202.3 $\pm$ 18.5	192.8 $\pm$ 16.0	<0.001

Data are presented as the mean $\pm$ standard deviation unless otherwise specified. AD – Alzheimer's disease; MCI – mild cognitive impairment; IOP – intraocular pressure; BCVA – Best-Corrected Visual Acuity; VDD – vertical disc diameter; HDD – horizontal disc diameter; MMSE – Mini-Mental Status Examination; RNFL – retinal nerve fiber layer; CCT – central corneal thickness.

locations (superior, central, and inferior) were significantly larger in the melatonin treated group than in the placebo group.

## Discussion

AD patients always suffer from serious dementia, memory loss, and cognitive dysfunction. Mild cognitive impairment (MCI) is

recognized as the transitory state between normality and AD dementia. Retina is a peripheral component of the central neural system. The anatomical and physiological features of the retina share many commonalities with the brain. These features collectively make the physical examination of the retina an effective, safe, and economic approach for evaluating brain lesions [36,37]. In the past decades, retinal imaging has been developed into a non-invasive method to assess the optic

**Table 5.** Hippocampal volumes and LCT data in melatonin group and placebo group.

	Melatonin (n=40)	Placebo (n=39)	P value
Hippocampus			
Total (mm <sup>3</sup> )	6.71±0.39	6.49±0.32	<0.001
Right (mm <sup>3</sup> )	3.38±0.31	3.27±0.21	<0.001
Left (mm <sup>3</sup> )	3.36±0.29	3.21±0.22	<0.001
CSF			
Pressure (mmHg)	13.3±2.1	13.5±2.3	P=0.38
Aβ1–42 (pg/mL)	329.62±117.59	310.82±118.66	<0.001
T-tau (pg/mL)	95.05±22.94	108.29±17.60	<0.001
P-tau181P (pg/mL)	38.27±13.80	45.08±12.73	<0.001
LCT (μm)			
Superior	206.91±14.55	195.29±15.10	<0.001
Central	246.83±16.02	238.50±13.79	<0.001
Inferior	220.54±15.16	205.08±14.21	<0.001
Average	226.89±16.02	215.42±15.28	<0.001
LCD (μm)	435.80±70.18	432.65±68.24	0.76

Data are presented as the mean±standard deviation unless otherwise specified. Aβ1–42 – amyloid β1–42; CSF – cerebrospinal fluid; LCD – lamina cribrosa depth; LCT – lamina cribrosa thickness.

nerve axons and central neural system [38]. A pioneering study demonstrated that the macular volume of AD patient is significantly smaller than that in healthy controls [16]. Another study showed that the RNFL thickness reduced significantly in AD patients, providing a potential diagnostic marker of the nervous system axonal loss [39]. Herein, we analyze the hippocampal volume and LC thickness in the MCI patients, and compare these data with the healthy controls. We show that these MCI patients have smaller LCT compared with the healthy controls. To our knowledge, this is the first study to verify the relationship between hippocampal volume and LCT in these MCI patients. Furthermore, the melatonin treatment can preserve the LCT and reduce the CSF T-tau level in the MCI patients. Dietary melatonin therapy would provide an effective medication for these MCI patients with LCT alterations. The RNFL is composed of axon bundles that originate from RGCs. RNFL is located just under the innermost neural layer of the retina surface. On the other hand, the choroid is composed of vascular structure and plays a critical role in the pathogenesis of various retinopathies [40]. Thus, examination of the RNFL and choroid is helpful for the diagnosis and monitoring of eye diseases. A previous study found significant RGC loss and reduced RNFL thickness in these AD patients [41]. RNFL thinning was also detected in these patients with dementia of Lewy bodies [42]. This evidence indicates a close relationship between retinal degeneration and AD pathology. The RNFL and choroid

thickness increase significantly after melatonin therapy, suggesting that melatonin also exerts beneficial effects on the retina and choroid of MCI patients.

LC is composed of extracellular matrix and multiple cellular components (such as astrocytes and microglia cells). Generally, LC affords structural and metabolic support to optic nerve fibers. LC degeneration is found both in the physiologic aging or pathologic conditions [43]. The present study showed that LCT is closely correlated with the hippocampal volume in MCI patients, thereby affording an effective diagnostic marker for these disorders. The data of hippocampal atrophy agree well with a previous study and is considered as a marker of the progression in MCI patients [44]. In clinical practice, diagnostic criteria are insufficient to discriminate MCI from other causes of dementia [45]. Thus, some ancillary methods are necessary for the diagnosis of MCI. Emerging studies intend to measure the level of amyloid deposition in central nervous system via detecting structural alteration in the optic disc. In postmortem analyses, tau, Aβ plaques, ubiquitin, and α-synuclein were studied, revealing correlation to disease severity [46]. It has been proposed that increased tau protein promotes the neurodegeneration process, predisposing laminar astrocytes to degeneration and results in a decreased LCT [47]. In this study, the up-regulated T-tau level was correlated with the reduced LCT in MCI patients. Since the CSF tau can influence the stability of



the cytoskeleton of laminar astrocytes, the LCT may serve as a potential indicator for alterations of the CSF tau level [48]. Generally, the biomarkers are not appropriate for clinical practice as they are expensive, invasive, and time-consuming. Thus, non-invasive methods such as retina examination have become a focus of interest with promising results [49]. These findings highlight the possibility that LCT may serve as a candidate marker for the impaired cognitive function.

Neuromarkers include a series of functional and chemical indicators to facilitate the diagnosis of AD and MCI. Functional neuromarkers are brain metabolic activities and electrical activities which can be detected by means of neuroimaging (e.g., EEG and ERP) at millisecond time resolution [50]. These functional neuromarkers are effective for creating specific patterns of brain changes and signal communication. They are also used to monitor the results of treatment by protocols of neuromodulation. EEG and MEG provide economical, non-invasive tools for the diagnosis of AD and studying disease progression, and they open a fresh view to cognitive decline from a network perspective [51]. Furthermore, these chemical indicators also provide safe biomarkers for diagnosis, prognosis, and evaluation of therapeutic responses of AD and MCI [52,53]. These chemical indicators play significant roles in the signal transmission of axonal pathways. In particular, melatonin may act as a candidate neuromarker for AD and MCI. Melatonin is a circadian neurohormone that modulates the brain activity in endocrine manner [54]. Both melatonin deficiency and synaptic injury have been found in the initial stages of AD [55]. Clinical trials have shown that the melatonin level of AD patients was reduced significantly, which makes the brain neurons more vulnerable to oxidative stress [56]. Research studies have proposed that the melatonin shortage may be related to plaque formation in the brain [57]. On the other hand, melatonin can mitigate the amyloid precursor protein (APP) formations and fibril production in AD patients [58]. Melatonin is reported to exert beneficial effects on the hippocampus and inhibits mitochondrial impairments in a rat model of AD [59]. Melatonin supplementation alleviates chronobiological symptoms such as sundowning and agitation and confusion in AD patients [60]. These beneficial potencies are thought to prevent neuronal loss and improve cognitive processes in AD and MCI patients. Herein, we show that dietary melatonin supplements can alleviate the LCT reduction in the MCI patients. The elevated IOP has been recognized as a critical risk factor for the LC damages in patients. On the other hand, several lines of evidences show that melatonin and analogues are effective in decreasing IOP in hypertensive eyes. As a well-known antioxidant, melatonin is not only able to scavenge free radicals directly, but also can enhance the production of endogenous anti-oxidative enzymes [61]. Thus, melatonin may protect the extracellular matrix and cellular components of LC (such as astrocytes and microglia cells) from oxidative insults. This might

be the underlying mechanism that is responsible for the melatonin-mediated protection on LC.

LC plays a critical role in preserving the morphological integrity of nerve fibers, and in transmitting neurotrophic factors sent from the upper centers to RGCs [62,63]. In AD patients, impaired astrocyte functions may cause structural changes in the LC similar to the pathological conditions in glaucoma [64]. Moreover, the RGC axons are vulnerable to mechanical insults. The LC defects that occur during the progression of neurodegeneration may hinder the transmission of neurotrophic factors to RGCs, causing disturbances of RGCs functions [65]. It has been shown that the laminar region of the ONH is extremely vulnerable during axonal loss [66]. However, it is unclear whether LC thinning is due to either physiological aging or pathophysiological aging. A pioneering study showed that LC is thinner in AD patients with higher tau protein level in CSF [48]. Another study showed that injecting A $\beta$  binding protein in patients with MCI could enhance the level of inclusion cells in retina [67]. We expanded these findings by studying the LCT and comparing hippocampus volume in MCI patients. These findings may be helpful to demonstrate correlation between cerebral and retinal damages.

In the past decade, developments in imaging modalities afford a unique opportunity to examine the LC architectures *in vivo* [68]. SD-OCT is capable of detecting early onset histopathological changes in the LC, such as the reduced thickness and posterior displacement of the LC. SD-OCT is efficient to capture the focal LC defects because it can differentiate the artifacts from actual LC defects due to vascular shadowing [69]. Therefore, we performed LC measurements via the SD-OCT and analyze the *in vivo* images. Volumetric measurement of several cerebral structures by using advanced neuroimaging techniques have become a method used for diagnosis and prognosis of neurodegeneration [70]. MRI in combination with software calculating brain volumes allows us to conduct unique investigations on brain structures and their functions [71]. In this study, we performed volumetric measurement for hippocampus after processing and correlated results with LCT which may be a potential prognostic marker. The hippocampus is pivotal for human learning and memory. It also plays a critical role in the subcortical networks to control the electrical activity of brain [72]. Generally, the hippocampus does not work in isolation, but connects extensively with other brain regions [73]. The hippocampus is well known to suffer from the structural degeneration with age, because it is a stress-susceptible region in the brain. A typical brain abnormality in AD is the reduced hippocampus volume. The reduction in hippocampus volume is believed to impair the learning and memory function of patients [74]. The hippocampus is more reliable than other structures for predicting the progressive course of MCI to AD in volumetric measurement [75].

Accordingly, commencement of disease-modifying agents at an early phase is important in order to prevent progression. Researchers have proposed that hippocampus atrophy could be used as a marker for progression of MCI to AD. Therefore, the *in vivo*, non-invasive assessment would be helpful for the diagnosis and prognosis of patients with MCI.

Admittedly, there were some limitations in our study such as the relatively small sample size. Moreover, our study was also limited by the fact that the MCI diagnosis was made according to clinical and MRI findings without using specific tests such as positron emission tomography (PET) scan which will show amyloid accumulation. Another limitation is that we did not include more patients with different types of MCI to perform a comparative analysis. Further larger scale studies with longer follow-up profiles are necessary to validate these findings.

## References:

- Migliaccio R, Agosta F, Possin KL et al: Mapping the progression of atrophy in early and late-onset Alzheimer's disease. *J Alzheimers Dis*, 2015; 46: 351–64
- Sheelakumari R, Kesavadas C, Lekha VS et al: Structural correlates of mild cognitive impairment: A clinicovolumetric study. *Neurol India*, 2018; 66: 370–76
- Honer WG, Ramos-Miguel A, Alamri J et al: The synaptic pathology of cognitive life. *Dialogues Clin Neurosci*, 2019; 21(3): 271–79
- Hart NJ, Koronyo Y, Black KL, Koronyo-Hamaoui M: Ocular indicators of Alzheimer's: Exploring disease in the retina. *Acta Neuropathol*, 2016; 132(6): 767–87
- Carelli V, La Morgia C, Ross-Cisneros FN, Sadun AA: Optic neuropathies: The tip of the neurodegeneration iceberg. *Hum Mol Genet*, 2017; 26(R2): R139–50
- Dong A, Toledo JB, Honnorat N et al: Heterogeneity of neuroanatomical patterns in prodromal Alzheimer's disease: Links to cognition, progression and biomarkers. *Brain*, 2017; 140: 735–47
- Tao Y, Geng L, Wang L et al: Use of hydrogen as a novel therapeutic strategy against photoreceptor degeneration in retinitis pigmentosa patients. *Med Sci Monit*, 2016; 22: 776–79
- Masland RH: The fundamental plan of the retina. *Nat Neurosci*, 2001; 4(9): 877–86
- Jenkins TM, Toosy AT: Optic neuritis: The eye as a window to the brain. *Curr Opin Neurol*, 2017; 30(1): 61–66
- Biscetti L, Luchetti E, Vergaro A et al: Associations of Alzheimer's disease with macular degeneration. *Front Biosci*, 2017; 9: 174–91
- Moghim S, Mazloumi M, Johari M et al: Evaluation of lamina cribrosa and choroid in nonglaucomatous patients with pseudoexfoliation syndrome using spectral-domain optical coherence tomography. *Invest Ophthalmol Vis Sci*, 2016; 57(3): 1293–300
- Eraslan M, Cerman E, Yildiz Balci S et al: The choroid and lamina cribrosa is affected in patients with Parkinson's disease: Enhanced depth imaging optical coherence tomography study. *Acta Ophthalmol*, 2016; 94(1): e68–75
- Mistry V, An D, Barry CJ et al: Association between focal lamina cribrosa defects and optic disc haemorrhage in glaucoma. *Br J Ophthalmol*, 2020; 104(1): 98–103
- Tao Y, Li C, Yao A et al: Intranasal administration of erythropoietin rescues the photoreceptors in degenerative retina: A noninvasive method to deliver drugs to the eye. *Drug Deliv*, 2019; 26(1): 78–88
- Ren R, Yang H, Gardiner SK et al: Anterior lamina cribrosa surface depth, age, and visual field sensitivity in the Portland Progression Project. *Invest Ophthalmol Vis Sci*, 2014; 55(3): 1531–39
- Ascaso FJ, Cruz N, Modrego PJ et al: Retinal alterations in mild cognitive impairment and Alzheimer's disease: An optical coherence tomography study. *J Neurol*, 2014; 261(8): 1522–30
- Tan CC, Yu JT, Tan L: Biomarkers for preclinical Alzheimer's disease. *J Alzheimers Dis*, 2014; 42(4): 1051–69
- Kropotov JD: Functional neuromarkers for neuropsychology. *Acta Neuropsychologica*, 2018; 16(1): 1–7
- Horvath A, Szucs A, Csukly G et al: EEG and ERP biomarkers of Alzheimer's disease: A critical review. *Front Biosci (Landmark Ed)*, 2018; 23: 183–220
- Yang S, Bornot JMS, Wong-Lin K, Prasad G: M/EEG-based biomarkers to predict the mild cognitive impairment and Alzheimer's disease: A review from the machine learning perspective. *IEEE Trans Biomed Eng*, 2019; 66(10): 2924–35
- Bruña R, Poza J, Gómez C et al: Analysis of spontaneous MEG activity in mild cognitive impairment and Alzheimer's disease using spectral entropies and statistical complexity measures. *J Neural Eng*, 2012; 9(3): 036007
- Jelles B, Scheltens P, van der Flier WM et al: Global dynamical analysis of the EEG in Alzheimer's disease: Frequency-specific changes of functional interactions. *Clin Neurophysiol*, 2008; 119(4): 837–41
- Rossini PM, Del Percio C, Pasqualetti P et al: Conversion from mild cognitive impairment to Alzheimer's disease is predicted by sources and coherence of brain electroencephalography rhythms. *Neuroscience*, 2006; 143(3): 793–803
- Howe AS, Bani-Fatemi A, De Luca V: The clinical utility of the auditory P300 latency subcomponent event-related potential in preclinical diagnosis of patients with mild cognitive impairment and Alzheimer's disease. *Brain Cogn*, 2014; 86: 64–74
- Baker KG: Evaluation of DSM-5 and IWG-2 criteria for the diagnosis of Alzheimer's disease and dementia with Lewy bodies. *Diagnosis (Berl)*, 2016; 3(1): 9–12
- Zuev VA, Trifonov NI, Linkova NS, Kvetnaia TV: Melatonin as a molecular marker of age-related pathologies. *Adv Gerontol*, 2017; 30(1): 62–69
- Zhou JN, Liu RY, Kamphorst W et al: Early neuropathological Alzheimer's changes in aged individuals are accompanied by decreased cerebrospinal fluid melatonin levels. *J Pineal Res*, 2003; 35(2): 125–30
- Brunner P, Sözer-Topcular N, Jockers R et al: Pineal and cortical melatonin receptors MT1 and MT2 are decreased in Alzheimer's disease. *Eur J Histochem*, 2006; 50(4): 311–16
- Sulkava S, Muggalla P, Sulkava R et al: Melatonin receptor type 1A gene linked to Alzheimer's disease in old age. *Sleep*, 2018; 41(7)
- Del Sole MJ, Sande PH, Fernandez DC et al: Therapeutic benefit of melatonin in experimental feline uveitis. *J Pineal Res*, 2012; 52(1): 29–37
- Sande PH, Dorfman D, Fernandez DC et al: Treatment with melatonin after onset of experimental uveitis attenuates ocular inflammation. *Br J Pharmacol*, 2014; 171(24): 5696–707
- Siu AW, Reiter RJ, To CH: Pineal indoleamines and vitamin E reduce nitric oxide-induced lipid peroxidation in rat retinal homogenates. *J Pineal Res*, 1999; 27(2): 122–28

## Conclusions

Non-invasive measurements such as OCT examination are helpful for the diagnosis of MCI. Dietary melatonin therapy can preserve the LCT, while reducing the CSF T-tau level of MCI patients. These data enrich our understandings about melatonin and shed light on developing an effective medication for MCI patients with LC alterations.

## Conflicts of interests

None.

33. Ting SK, Hameed S, Earnest A, Tan EK: Dissociative semantic breakdown in Alzheimer's disease: Evidence from multiple category fluency test. *Clin Neurol Neurosurg*, 2013; 115(7): 1049–51
34. Folstein MF, Folstein SE, McHugh PR: "Mini-Mental State", A practical method for grading the cognitive state of patients for the clinician. *J Psychiatr Res*, 1975; 12: 189–98
35. Manjón JV, Coupé P: VolBrain: An online MRI brain volumetry system. *Front Neuroinform*, 2016; 10: 30
36. Erskine L, Herrera E: Connecting the retina to the brain. *ASN Neuro*, 2014; 6(6): pii: 1759091414562107
37. Kirschfeld K: How we perceive our own retina. *Proc Biol Sci*, 2017; 284(1865): pii: 20171904
38. Pichi F, Sarraf D, Arepalli S et al: The application of optical coherence tomography angiography in uveitis and inflammatory eye diseases. *Prog Retin Eye Res*, 2017; 59: 178–201
39. Cunha JP, Proença R, Dias-Santos A et al: OCT in Alzheimer's disease: Thinning of the RNFL and superior hemiretina. *Graefes Arch Clin Exp Ophthalmol*, 2017; 255(9): 1827–35
40. Yazdani S, Samadi P, Pakravan M et al: Peripapillary RNFL thickness changes after panretinal photocoagulation. *Optom Vis Sci*, 2016; 93: 1158–62
41. den Haan J, Verbraak FD, Visser PJ, Bouwman FH: Retinal thickness in Alzheimer's disease: A systematic review and meta-analysis. *Alzheimers Dement (Amst)*, 2017; 6: 162–70
42. Moreno-Ramos T, Benito-León J, Villarejo A, Bermejo-Pareja F: Retinal nerve fiber layer thinning in dementia associated with Parkinson's disease, dementia with Lewy bodies, and Alzheimer's disease. *J Alzheimers Dis*, 2013; 34(3): 659–64
43. Jonas JB, Berenshtein E, Holbach L: Lamina cribrosa thickness and spatial relationships between intraocular space and cerebrospinal fluid space in highly myopic eyes. *Invest Ophthalmol Vis Sci*, 2004; 45(8): 2660–65
44. Fox NC, Ridgway GR, Schott JM: Algorithms, atrophy and Alzheimer's disease: Cautionary tales for clinical trials. *Neuroimage*, 2011; 57: 15–18
45. Tsuang D, Leverenz JB, Lopez OL et al: APOE ε4 increases risk for dementia in pure synucleinopathies. *JAMA Neurol*, 2013; 70: 223–28
46. Beach TG, Kuo YM, Spiegel K et al: The cholinergic deficit coincides with Abeta deposition at the earliest histopathologic stages of Alzheimer's disease. *J Neuropathol Exp Neurol*, 2000; 59: 308–13
47. Kirbas S, Turkyilmaz K, Anlar O et al: Retinal nerve fiber layer thickness in patients with Alzheimer disease. *J Neuroophthalmol*, 2013; 33: 58–61
48. Kayabasi U, Sergott R, Rispoli M: Retinal examination for the diagnosis of Alzheimer's disease. *Int J Ophthalmic Pathol*, 2014; 3: 4–7
49. Lee EJ, Kim TW, Lee DS et al: Increased CSF tau level is correlated with decreased lamina cribrosa thickness. *Alzheimers Res Ther*, 2016; 8: 6
50. McMackin R, Bede P, Pender N et al: Neurophysiological markers of network dysfunction in neurodegenerative diseases. *Neuroimage Clin*, 2019; 22: 101706
51. Cottreau BR, Ales JM, Norcia AM: How to use fMRI functional localizers to improve EEG/MEG source estimation. *J Neurosci Methods*, 2015; 250: 64–73
52. Hartmann S, Ledur Kist TB: A review of biomarkers of Alzheimer's disease in noninvasive samples. *Biomark Med*, 2018; 12(6): 677–90
53. Ghidoni R, Squitti R, Siotto M, Benussi L: Innovative biomarkers for Alzheimer's Disease: Focus on the hidden disease biomarkers. *J Alzheimers Dis*, 2018; 62(4): 1507–18
54. Sanchez-Barcelo EJ, Rueda N, Mediavilla MD et al: Clinical uses of melatonin in neurological diseases and mental and behavioural disorders. *Curr Med Chem*, 2017; 24(35): 3851–78
55. Shi Y, Fang YY, Wei YP et al: Melatonin in synaptic impairments of Alzheimer's disease. *J Alzheimers Dis*, 2018; 63(3): 911–26
56. Shukla M, Govitrapong P, Boontem P et al: Mechanisms of melatonin in alleviating Alzheimer's disease. *Curr Neuropharmacol*, 2017; 15(7): 1010–31
57. Poegele B, Miravalle L, Zagorski MG et al: Melatonin reverses the profibrillogenic activity of apolipoprotein E4 on the Alzheimer amyloidAbeta peptide. *Biochemistry*, 2001; 40(49): 14995–5001
58. Gunata M, Parlakpinar H, Acet HA: Melatonin: A review of its potential functions and effects on neurological diseases. *Rev Neurol (Paris)*, 2020; 176(3): 148–65
59. Paradies G, Petrosillo G, Paradies V et al: Melatonin, cardiolipin and mitochondrial bioenergetics in health and disease. *J Pineal Res*, 2010; 48(4): 297–310
60. Brusco LI, Márquez M, Cardinali DP: Melatonin treatment stabilizes chronobiologic and cognitive symptoms in Alzheimer's disease. *Neuro Endocrinol Lett*, 2000; 21(1): 39–42
61. Crooke A, Huete-Toral F, Colligris B, Pintor J: The role and therapeutic potential of melatonin in age-related ocular diseases. *J Pineal Res*, 2017; 63(2)
62. Rodriguez C, Mayo JC, Sainz RM et al: Regulation of antioxidant enzymes: A significant role for melatonin. *J Pineal Res*, 2004; 36(1): 1–9
63. Inoue R, Hangai M, Kotera Y et al: Three-dimensional high-speed optical coherence tomography imaging of lamina cribrosa in glaucoma. *Ophthalmology*, 2009; 116(2): 214–22
64. Snyder PJ, Johnson LN, Lim YY et al: Nonvascular retinal imaging markers of preclinical Alzheimer's disease. *Alzheimers Dement (Amst)*, 2016; 4: 169–78
65. Hernandez MR: The optic nerve head in glaucoma: Role of astrocytes in tissue remodeling. *Prog Retin Eye Res*, 2000; 19: 297–321
66. Lambert WS, Clark AF, Wordinger RJ: Neurotrophin and Trk expression by cells of the human lamina cribrosa following oxygen-glucose deprivation. *BMC Neurosci*, 2004; 5: 51
67. Kirbas S, Turkyilmaz K, Anlar O et al: Retinal nerve fiber layer thickness in patients with Alzheimer disease. *J Neuroophthalmol*, 2013; 33: 58–61
68. Zabel P, Kałużny JJ, Wiłkość-Dębczyńska M et al: Peripapillary retinal nerve fiber layer thickness in patients with Alzheimer's disease: A comparison of eyes of patients with Alzheimer's disease, primary open-angle glaucoma, and preperimetric glaucoma and healthy controls. *Med Sci Monit*, 2019; 25: 1001–8
69. Cakmak S, Altan C, Topcu H et al: Comparison of the lamina cribrosa measurements obtained by spectral-domain and swept-source optical coherence tomography. *Curr Eye Res*, 2019; 44(9): 968–74
70. Oishi K, Faria A, Jiang H et al: Atlas-based whole brain white matter analysis using large deformation diffeomorphic metric mapping: Application to normal elderly and Alzheimer's disease participants. *Neuroimage*, 2009; 46: 486–99
71. Acer N, Bastepe-Gray S, Sagiroglu A et al: Diffusion tensor and volumetric magnetic resonance imaging findings in the brains of professional musicians. *J Chem Neuroanat*, 2018; 88: 33–40
72. Fares J, Bou Diab Z, Nabha S, Fares Y: Neurogenesis in the adult hippocampus: History, regulation, and prospective roles. *Int J Neurosci*, 2019; 129(6): 598–611
73. Gruber MJ, Ranganath C: How curiosity enhances hippocampus-dependent memory: The prediction, appraisal, curiosity, and exploration (PACE) framework. *Trends Cogn Sci*, 2019; 23(12): 1014–25
74. Giuliano A, Donatelli G, Cosottini M et al: Hippocampal subfields at ultra-high field MRI: An overview of segmentation and measurement methods. *Hippocampus*, 2017; 27(5): 481–94
75. Frost S, Guymer R, Aung KZ et al: Alzheimer's disease and the early signs of age-related macular degeneration. *Curr Alzheimer Res*, 2016; 13: 1259–66